COMMUNICATION

Ultralow-Threshold Laser Realized in Zinc Oxide

By *Hai Zhu, Chong-Xin Shan,* Bin Yao, Bing-Hui Li, Ji-Ying Zhang, Zheng-Zhong Zhang, Dong-Xu Zhao, De-Zhen Shen, Xi-Wu Fan, You-Ming Lu,* and *Zi-Kang Tang*

Short-wavelength semiconductor lasers have attracted much attention since the demonstration of laser diodes in ZnSe and GaN.[1,2] The attention derives mainly from the versatile applications of this type of lasers in data storage, display, communication, lighting, and medical fields. Zinc oxide (ZnO) has a wide bandgap (3.37 eV) and a large exciton-binding energy (60 meV), which is much larger than that of ZnSe (22 meV) and GaN (25 meV), suggesting that high-efficiency low-threshold light-emitting devices or laser diodes operating at room or even higher temperatures can be realized.[3–8] However, up to now most of the lasing actions in ZnO have been demonstrated by optical pumping,[9–12] while the reports on electrically pumped lasing are very scarce, even though lasing from ZnO by electrical excitation is highly desirable.[13–15] Leong et al. have demonstrated electrically pumped lasing in ZnO/SiO_2 nanocomposites sandwiched by p-SiC or p-GaN and n-ZnO:Al.[13,14] Moreover, electrically pumped lasers have also been observed in $Au/SiO_x/$ZnO metal–insulator–semiconductor structures.[15] However, the above-mentioned cases are all random lasers, whose poor directionality and controllability are known to impair their usefulness.[12,16] Up to date and to the best of our knowledge, only one report has shown electric-driven Fabry–Pérot resonant lasing in ZnO, and it was realized in a ZnBeO-based p–n junction.[17] Since reliable and stable p-doping of ZnO is still a challenge, realizing such a p–n junction in ZnBeO, which has larger band gap, is not expected by most researchers. Additionally, the biotoxicity of beryllium renders this material less desirable. To avoid the difficulties in p-type doping of ZnO, p-GaN has been employed by some groups to form p–n junctions with n-ZnO in light-emitting devices, in virtue of their similarity in crystalline structure and closely matched lattice constant.[18–21] However, the electroluminescence (EL) spectra of ZnO/GaN heterojunctions usually show strong emissions from the GaN layer, while that from the ZnO layer is very weak or even undetectable.[18,19] In that case, p-GaN does not supply holes to n-ZnO; contrarily, ZnO acts as an electron source for the GaN layer. Thus, the advantage of large exciton-binding energy of ZnO is not fully exploited. A MgO layer has been used to block the electrons in the ZnO layer, and EL emission from ZnO has been observed by our group.[19]

In this paper, by properly engineering the band alignment of n-ZnO/p-GaN heterojunctions using a dielectric MgO layer, most of the electrons are shown to be confined in the ZnO layer, while holes can be injected into the ZnO layer from the p-GaN. In this way, continuous-current-driven lasers in ZnO have been obtained. The threshold current of the laser is only 0.8 mA, the smallest value ever reported for blue-/ultraviolet-light semiconductor laser diodes to the best of our knowledge.

The surface morphology of the ZnO layer is shown in Figure 1a. The layer is composed of closely packed quasi-hexagon-shaped columns with average size of about 100 nm. Note that the top surface of the columns shows a smooth ZnO (0001) natural facet. The appearance of this facet suggests that each column is of high crystalline quality. Figure 1b shows the room-temperature photoluminescence (PL) spectra of the ZnO and GaN layers. As shown, the spectrum of ZnO displays a dominant sharp near-band-edge (NBE) emission at 378 nm and a very weak deep-level emission at around 550 nm. The spectrum of the p-GaN is dominated by a broad peak centered at about 450 nm, which is frequently observed in Mg-doped p-GaN, and can be attributed to transitions between conduction-band electrons or donors and Mg-related acceptors.[22] The fringes observed in the spectrum are due to the interference between GaN/air and the sapphire/GaN interfaces.

Figure 2a shows the EL spectra of the heterojunction with and without a MgO dielectric layer (marked by A and B, respectively) under the same injection current (curve B has been magnified 70 times for comparison). Without the MgO layer, the spectrum exhibits a broad peak centered at 530 nm and a weak one at 445 nm. The former comes from the deep-level emission in ZnO, while the latter originates from the GaN layer. With the MgO layer, only one peak at approximately 400 nm can be observed, and the intensity of the peak is almost two orders of magnitude higher than that of the heterojunction without the MgO layer. This peak has been observed frequently in the EL spectra of ZnO-based hetero- and homojunctions, and is generally attributed to the donor–acceptor pair recombination in ZnO.[4,14,23–25] The effect of the MgO dielectric layer on the EL spectrum of the

[*] Prof. C.-X. Shan, H. Zhu, B. Yao, B.-H. Li, J.-Y. Zhang, Z.-Z. Zhang, D.-X. Zhao, D.-Z. Shen, X.-W. Fan
Lab of Excited State Processes
Changchun Institute of Optics
Fine Mechanics and Physics
Chinese Academy of Sciences
Changchun 130033 (P. R. China)
E-mail: phycxshan@yahoo.com.cn

H. Zhu
Graduate School of the Chinese Academy of Sciences
Beijing 100049 (P. R. China)

Prof. Y.-M. Lu
College of Materials Science and Engineering
Shenzhen University
Shenzhen 518060 (P. R. China)

Prof. Z.-K. Tang
Department of Physics
Hong Kong University of Science & Technology
Clear Water Bay, Kowloon
Hong Kong (P. R. China)

DOI: 10.1002/adma.200802907

© 2009 WILEY-VCH Verlag GmbH & Co. KGaA, Weinheim
WILEY InterScience DISCOVER SOMETHING GREAT

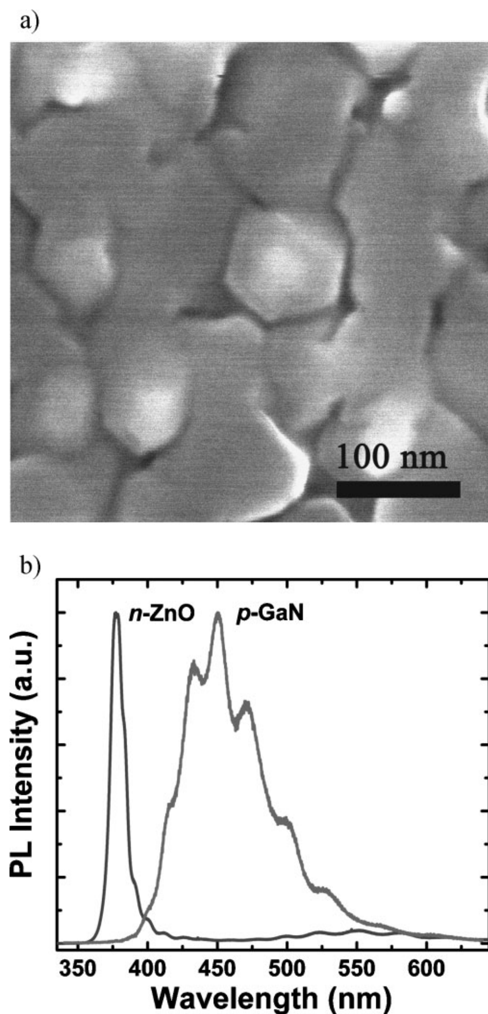

Figure 1. a) SEM image of the ZnO layer, revealing that the ZnO layer is composed of columns with smooth top surfaces. b) Normalized room-temperature PL spectra of the n-ZnO and p-GaN layer.

heterojunction can be understood in terms of the band alignment, as illustrated in Figure 2b. Without the dielectric layer, electrons will drift from ZnO to GaN, while holes drift from GaN to ZnO under forward bias. In this case, carrier radiative recombination will occur in the depletion area near the p–n junction. As a result, emissions from both GaN and ZnO layers can be detected. Since there should be many structural defects at the II–VI/III–V interface, only deep-level emissions are observed in both layers. The situations are different with the presence of the MgO dielectric layer. Under forward bias, most of the voltage will be applied on the MgO layer, because of its dielectric nature. Therefore, the bands of MgO will bend. Consequently, holes in the GaN layer can tunnel through the barrier and enter into the ZnO layer, because the effective barrier in the vicinity of valence band offset (VBO) is greatly reduced due to band bending, while electrons will be confined in the ZnO layer by the large conduction-band offset (CBO) between ZnO and MgO, as shown in Figure 2b. Due to the depletion of electrons, the emission from GaN is almost undetectable, while the emission from the ZnO

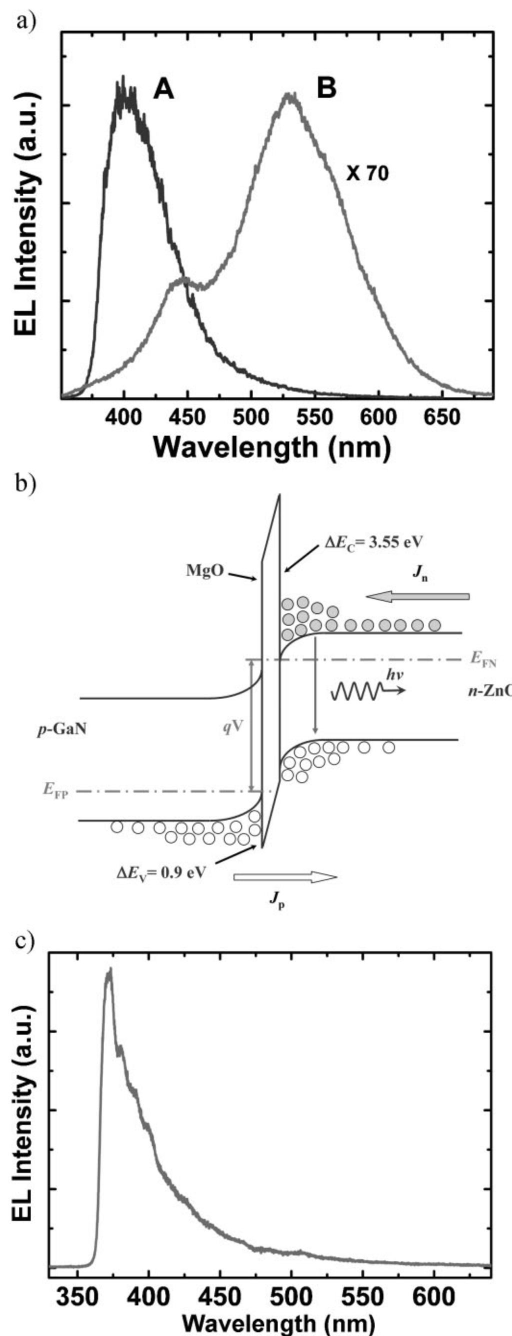

Figure 2. a) EL spectra of the n-ZnO/p-GaN heterojunction with (curve A) and without (curve B) MgO dielectric layer under the same injection current (note that the intensity of curve B has been magnified by 70 times). b) Schematic diagram showing the band alignment of the n-ZnO/MgO/p-GaN heterojunction under forward bias. The large CBO will confine electrons in the ZnO layer, while holes can tunnel through the relatively small effective barrier and enter into the ZnO layer from the GaN layer. c) EL spectrum of the heterojunction under reverse bias, confirming the electron-blocking role of the MgO layer.

layer has been remarkably enhanced with the holes ''borrowed'' from the p-GaN layer, in addition to the accumulated electrons. In order to confirm the origin of the emission at about 400 nm, reverse bias was applied to the heterojunction. Under reverse bias, it is expected that electrons in the GaN layer will be blocked

WILEY InterScience® DISCOVER SOMETHING GREAT
© 2009 WILEY-VCH Verlag GmbH & Co. KGaA, Weinheim

by the MgO layer due to the large CBO, while holes in the ZnO layer can tunnel through the VBO and enter into the GaN layer. In this case, the emission from ZnO should be reduced, while that from GaN should be enhanced. Experimentally, the EL of the heterojunction under reverse bias has been recorded from the back face, and a typical spectrum is shown in Figure 2c. A dominant emission peak centered at about 370 nm, due to the NBE emission of GaN, is observed, while the emission from the ZnO layer is almost undetectable. The agreement between the experimental data and the predictions confirms that the MgO layer can indeed block electrons as expected, and the emission at around 400 nm observed under forward bias comes from the ZnO layer.

The schematic diagram and emission recording geometry of the n-ZnO/MgO/p-GaN diode is shown in Figure 3a, and the current–voltage (*I*–*V*) curve of the diode is illustrated in Figure 3b.

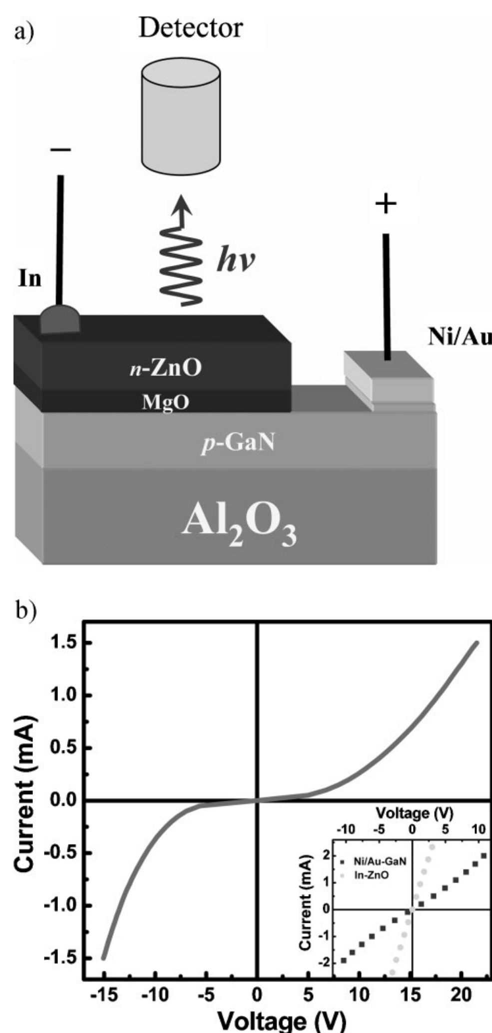

Figure 3. a) Schematic illustration of the diode structure and the recording geometry of the lasing action. b) *I*–*V* curve of the diode, revealing obvious rectifying behavior with a turn-on voltage of about 7 V. The inset shows the *I*–*V* curves of a Ni/Au electrode on the GaN layer and In electrode on the ZnO layer, showing that Ohmic contacts have been achieved for both electrodes.

Obvious rectifying behavior with a turn-on voltage of about 7 V is observed in the *I*–*V* curve. The linear curves for both Ni/Au on p-GaN and In on n-ZnO reveal that good Ohmic contacts have been obtained in both electrodes. The lasing characteristics of the heterojunction diode under the injection of continuous current are shown in Figure 4. By applying a forward bias onto the diode, the EL spectra are collected from the top face of the structure at room temperature. When the injection current is 0.66 mA, a broad spontaneous emission with a full-width at half-maximum (FWHM) of about 41 nm appears; when the current is increased to 1.04 mA, some very sharp peaks, superimposed on the broad spontaneous emission, are observed. With the current further increases to 1.22 mA, more such sharp peaks appear in a wide spectral range from 380 nm to 510 nm, and the sharp peaks become much more dominant. The FWHM of the sharp peaks is about 0.8 nm. The appearance of sharp peaks with very narrow FWHMs with increasing injection currents implies that lasing action has been obtained in ZnO. The dependence of the emission intensity of the diode on the injection current is shown in the inset of Figure 4a, from which a threshold current of 0.8 mA can be obtained. Note that the reported threshold currents in blue-/ultraviolet-light semiconductor laser diodes are usually tens or even hundreds of milliamperes,[26–29] two or three orders of magnitude larger than that realized in our diode. The spectra recorded from the edge of the structure shows only spontaneous emissions, while those from the top surface manifest lasing actions as shown in Figure 4b, indicating that the lasing in our ZnO diode is directionally normal to the substrate. A typical emission image of the diode taken from the ZnO side under an above-threshold current is shown in Figure 4c. Apart from the blue light from the whole junction area, some bright spots can also be observed in the image.

To realize electrically driven lasing, efficient carrier accumulation is necessary.[30] In our case, as depicted in Figure 2b, the MgO dielectric layer blocks the escape of the majority of carriers (electrons) in ZnO, meanwhile the majority of carriers (holes) in GaN can be efficiently injected into ZnO under forward bias. As a result, the emission in ZnO has been enhanced significantly. Another key point in the realization of lasing action may be the column structure of the ZnO layer. Since the refractive index of ZnO (2.45) is larger than that of air (1.0) and MgO (1.7), the smooth top surface of the small-sized ($\sim$100 nm) ZnO columns serves as a mirror that defines an optical microcavity.[31] However, it is difficult for us to calculate the effective cavity length from the spacing of the oscillation modes, because the spacing is strongly affected by the thickness or diameter fluctuations of the ZnO columns.[32] As for the ultralow threshold, the microcavity will strongly increase the coupling efficiency of spontaneous emission into lasing modes, and thus help to reduce the threshold.[33] Interestingly, the threshold of a random laser reported in ZnO nanoparticles driven by pulsed current is also very low (4.3 mA),[14] suggesting to us that the intrinsic characters of ZnO, such as large exciton-binding energies and high optical gain, may also contribute significantly to the ultralow threshold.[3]

In conclusion, continuous-current-driven lasers operating at room temperature have been realized in ZnO by integrating n-ZnO and p-GaN together with a dielectric MgO layer, which acted as an electron-blocking barrier. The threshold of this diode is about 0.8 mA, the smallest threshold for semiconductor laser

© 2009 WILEY-VCH Verlag GmbH & Co. KGaA, Weinheim
WILEY InterScience DISCOVER SOMETHING GREAT

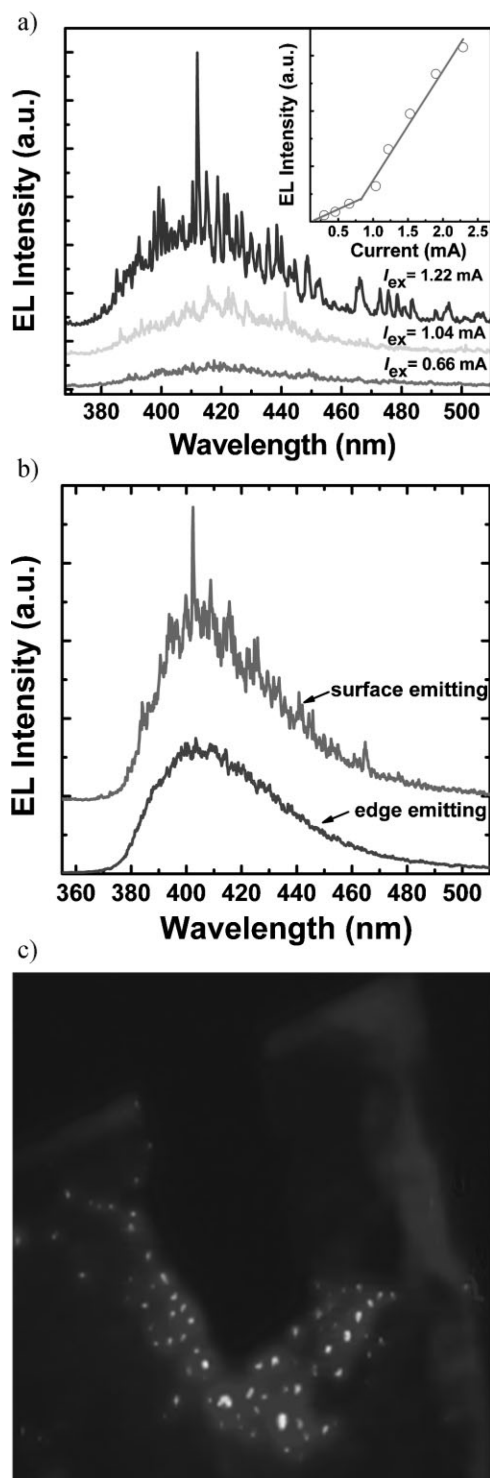

Figure 4. a) Three typical EL spectra of the diode under different currents. Note that the spectra were offset for comparison. The inset illustrates the emission intensity of the diode as a function of injection current. b) Emission spectra recorded from the top-surface and edge of the device above the threshold, revealing that the lasing is directionally normal to the substrate. c) Lasing emission image of the diode.

diodes operating in the blue/ultraviolet-light spectrum range to the best of our knowledge. The reason for the ultralow threshold may lie in the microcavities formed in the ZnO columns as well as the large exciton binding energy and high optical gain of the ZnO small-sized structures. The p-GaN used in this paper serves as a hole source for the ZnO, and we believe that similar results may be attainable by extending the hole source to other p-type materials with proper conduction- and valence-band offsets with ZnO.

Experimental

For the fabrication of the heterojunction diodes, undoped ZnO and MgO layers were deposited onto commercially available GaN/Al_2O_3 (0001) templates using a VG V80H plasma-assisted molecular-beam epitaxy system. The GaN layer presented p-type conduction, with a hole concentration and mobility of $3.0 \times 10^{17}\,cm^{-3}$ and $10\,cm^2\,V^{-1}\,s^{-1}$, respectively, and a thickness of about 2 μm. Prior to the growth, the GaN/Al_2O_3 templates were pretreated at 750 °C for 30 min to remove any possibly adsorbed contaminants and produce a clean surface. High-purity (6N) elemental zinc and magnesium were used as precursors for the ZnO and MgO growth, and the oxygen source used was radical O produced in a plasma cell working at 300 W. The pressure and temperature during the growth process were fixed at 1×10^{-3} Pa and 800 °C, respectively. First a 30 nm MgO layer, then a 300 nm ZnO layer were deposited onto the p-GaN film in sequence. The undoped ZnO showed n-type conduction with an electron concentration of $2.5 \times 10^{17}\,cm^{-3}$ and a mobility of $5\,cm^2\,V^{-1}\,s^{-1}$. For comparison, another heterojunction sample without a MgO layer was also prepared under the same conditions. Bilayer Ni/Au and monolayer In electrodes were employed as the contacts for p-GaN and n-ZnO layers, respectively. The electrical characteristics of the diodes were measured using a Lakeshore 7707 Hall measurement system. The morphology of the structure was characterized by scanning electron microscopy (SEM) using a Hitachi S4800 microscope. PL spectra of the diodes were recorded using a JY-630 micro-Raman spectrometer with the 325 nm line of a He–Cd laser as the excitation source. EL measurements were carried out in a Hitachi F4500 spectrometer, and a continuous-current power source was used to excite the diodes. Note that all the measurements were performed at room temperature.

Acknowledgements

This work is supported by the Key Project of NNSFC (50532050), the "973" program (2006CB604906 and 2008CB317105), The Knowledge Innovative Program of CAS (KJCX3.SYW.W01) and the NNSFC (10674133, 10774132, and 60776011). The authors would like to thank Prof. SK Hark for retouching the language of this paper.

Received: October 2, 2008
Revised: November 1, 2008
Published online: January 28, 2009

[1] M. A. Hasse, J. Qui, J. M. De Puydt, H. Cheng, *Appl. Phys. Lett.* **1991**, *59*, 1272.
[2] S. Nakamura, *Science* **1998**, *281*, 956.
[3] Z. K. Tang, G. K. L. Wong, P. Yu, M. Kawasaki, A. Ohtomo, H. Koinuma, Y. Segawa, *Appl. Phys. Lett.* **1998**, *72*, 3270.
[4] A. Tsukazaki, A. Ohtomo, T. Onuma, M. Ohtani, T. Makino, M. Sumiya, K. Ohtani, S. F. Chichibu, S. Fuke, Y. Segawa, H. Ohno, H. Koinuma, M. Kawasaki, *Nat. Mater.* **2005**, *4*, 42.
[5] D. C. Look, *Mater. Sci. Eng. B* **2001**, *80*, 383.

© 2009 WILEY-VCH Verlag GmbH & Co. KGaA, Weinheim

[6] S. J. Pearton, D. P. Norton, K. Ip, Y. W. Heo, T. Steiner, *Prog. Mater. Sci.* **2005**, *50*, 293.
[7] D. K. Hwang, M. S. Oh, J. H. Lim, S. J. Park, *J. Phys. D* **2007**, *40*, R387.
[8] S. J. Jiao, Z. Z. Zhang, Y. M. Lu, D. Z. Shen, B. Yao, J. Y. Zhang, B. H. Li, D. X. Zhao, X. W. Fan, Z. K. Tang, *Appl. Phys. Lett.* **2006**, *88*, 031911.
[9] M. H. Huang, S. Mao, H. Feick, H. Q. Yan, Y. Y. Wu, H. Kind, E. Weber, R. Russo, P. D. Yang, *Science* **2001**, *292*, 1897.
[10] P. Zu, Z. K. Tang, G. K. L. Wong, M. Kawasaki, A. Ohtomo, H. Koinuma, Y. Segawa, *Solid State Commun.* **1997**, *103*, 459.
[11] H. Cao, Y. G. Zhao, H. C. Ong, S. T. Ho, J. Y. Dai, J. Y. Wu, R. P. H. Chang, *Appl. Phys. Lett.* **1998**, *73*, 3656.
[12] H. Cao, Y. G. Zhao, H. C. Ong, R. P. H. Chang, *Phys. Rev. B* **1999**, *59*, 15107.
[13] E. S. P. Leong, S. F. Yu, *Adv. Mater.* **2006**, *18*, 1685.
[14] E. S. P. Leong, S. F. Yu, S. P. Lau, *Appl. Phys. Lett.* **2006**, *89*, 221109.
[15] X. Y. Ma, P. L. Chen, D. S. Li, Y. Y. Zhang, D. R. Yang, *Appl. Phys. Lett.* **2007**, *91*, 251109.
[16] D. S. Wiersma, *Nat. Phys.* **2008**, *4*, 359.
[17] Y. R. Ryu, J. A. Lubguban, T. S. Lee, H. W. White, T. S. Jeong, C. J. Youn, B. J. Kim, *Appl. Phys. Lett.* **2007**, *90*, 131115.
[18] Y. I. Alivov, J. E. Van Nostrand, D. C. Look, M. V. Chukichev, B. M. Ataev, *Appl. Phys. Lett.* **2003**, *83*, 2943.
[19] S. J. Jiao, Y. M. Lu, D. Z. Shen, Z. Z. Zhang, B. H. Li, J. Y. Zhang, B. Yao, Y. C. Liu, X. W. Fan, *Phys. Status Solidi C* **2006**, *4*, 972.
[20] R. W. Chuang, R. X. Wu, L. W. Lai, C. T. Lee, *Appl. Phys. Lett.* **2007**, *91*, 231113.
[21] D. J. Rogers, F. H. Teherani, A. Yasan, K. Minder, P. Kung, M. Razeghi, *Appl. Phys. Lett.* **2006**, *88*, 141918.
[22] S. Nakamura, T. Mukai, M. Senoh, *Jpn. J. Appl. Phys. Part 2* **1991**, *30*, L1998.
[23] Y. I. Alivov, Ü. Özgür, X. Gu, C. Liu, Y. Moon, H. Morkoc, O. Lopatiuk, L. Chernyak, C. W. Litton, *J. Electron. Mater.* **2007**, *36*, 409.
[24] Z. P. Wei, Y. M. Lu, D. Z. Shen, Z. Z. Zhang, B. Yao, B. H. Li, J. Y. Zhang, D. X. Zhao, X. W. Fan, Z. K. Tang, *Appl. Phys. Lett.* **2007**, *90*, 042113.
[25] L. J. Mandalapu, Z. Yang, S. Chu, J. L. Liu, *Appl. Phys. Lett.* **2008**, *92*, 122101.
[26] S. H. Yen, Y. K. Kuo, *Appl. Phys. Lett.* **2008**, *103*, 103115.
[27] K. Okamoto, H. Ohta, S. F. Chichibu, J. Ichihara, H. Takasu, *Jpn. J. Appl. Phys. Part 2* **2007**, *46*, L187.
[28] S. Nakamura, S. Pearton, G. Fasol, *The Blue Laser Diodes*, 2nd ed, Springer, Berlin **2000**.
[29] G. Fasol, *Science* **1996**, *272*, 1751.
[30] X. F. Duan, Y. Huang, R. Agarwal, C. M. Lieber, *Nature* **2003**, *421*, 241.
[31] A. V. Kavokin, J. J. Baumberg, G. Malpuech, F. P. Laussy, *Microvavities*, Oxford University Press, Oxford **2007**, p. 13.
[32] F. Koyama, *J. Light Technol.* **2006**, *24*, 4502.
[33] Y. Yamamoto, S. Machida, G. Bjork, *Phys. Rev. A* **1991**, *44*, 657.

© 2009 WILEY-VCH Verlag GmbH & Co. KGaA, Weinheim
WILEY InterScience® DISCOVER SOMETHING GREAT